Original Article

Peptidylarginine deiminase inhibition prevents diabetes development in NOD mice.

Running title: PAD inhibition protects NOD mice from diabetes

Fernanda M. C. Sodré[1], Samal Bissenova[1], Ylke Bruggeman[1], Ronak Tilvawala[2,3], Dana P. Cook[1], Claire Berthault[4], Santanu Mondal[2], Aïsha Callebaut[1], Sylvaine You[4], Raphael Scharfmann[4], Roberto Mallone[4,5], Paul R. Thompson[2], Chantal Mathieu[1], Mijke Buitinga[1*] and Lut Overbergh[1*#]

Author affiliations of Manuscript in preparation.

[1]Laboratory for Clinical and Experimental Endocrinology, KU Leuven, Leuven, Belgium
[2]Biochemistry and Molecular Pharmacology, University of Massachusetts Medical School, Worcester MA, USA
[3]Department of Molecular Biosciences, The university of Kansas, Lawerence, KS, USA
[4]Université de Paris, Institut Cochin, CNRS, INSERM, 75014 Paris, France.
[5]Assistance Publique Hôpitaux de Paris, Hôpitaux Universitaires de Paris Centre-Université de Paris, Cochin Hospital, Service de Diabétologie et Immunologie Clinique, 75014 Paris, France.

*Equal contribution senior authors
[#] Corresponding author:
Dr. Lut Overbergh
Lab Clin & Exp Endocrinology (CEE)
KU Leuven
Herestraat 49, O&N1, box 902
B-3000 Leuven
Belgium
Tel +32-16-37.74.66
Fax +32-16-34.60.35
Email lutgart.overbergh@kuleuven.be

Word count: 4240
Figure count: 7 figures
Key words: Type 1, NOD mice, Neutrophils, Prevention, T Cells

Abstract

Protein citrullination plays a role in several autoimmune diseases. Its involvement in murine and human type 1 diabetes has recently been recognized through the discovery of antibodies and T-cell reactivity against citrullinated peptides. In the current study, we demonstrate that systemic inhibition of peptidylarginine deiminases (PADs), the enzymes mediating citrullination, through BB-Cl-amidine treatment, prevents diabetes development in NOD mice. This prevention was associated with reduced levels of citrullination in the pancreas, decreased circulating autoantibody titers against citrullinated GRP78 and reduced spontaneous NETosis of bone marrow-derived neutrophils. Moreover, BB-Cl-amidine treatment induced a shift from Th1 to Th2 cytokines in the serum and an increase in the frequency of regulatory T cells in the blood and spleen. In the pancreas, BB-Cl-amidine treatment preserved insulin production and was associated with a less destructive immune infiltrate, characterized by reduced frequencies of effector memory $CD4^+$ T cells and a modest reduction in the frequency of IFNγ-producing $CD4^+$ and $CD8^+$ T cells. Our results point to a role of citrullination in the pathogenesis of autoimmune diabetes, with PAD inhibition leading to disease prevention through modulation of immune pathways. These findings provide insight in the potential of PAD inhibition for treating autoimmune diseases like type 1 diabetes.

Introduction

Emerging evidence demonstrates a role for post-translational modifications (PTMs) in the pathogenesis of type 1 diabetes (1–10). One of these PTMs is citrullination, the conversion of arginine into citrulline, mediated by peptidylarginine deiminases (PADs), of which 5 isozymes have been described (11). The loss of a positively charged arginine in peptides enhances their binding affinity to type 1 diabetes predisposing HLA-DR4 molecules (12,13) and may thereby elicit autoreactive T-cell responses. Indeed, it has been shown that autoreactive $CD4^+$ T cells of patients with type 1 diabetes recognize citrullinated GAD65 (4). Moreover, our group showed that citrullinated glucose regulated protein 78 (GRP78) is an autoantigen in NOD mice and in human type 1 diabetes (5,6,10). We also provided direct evidence for cytokine-induced citrullination of GRP78 in INS-1E beta-cells (5) and human islets (10), indicating that GRP78 can be citrullinated in beta-cells in the absence of immune cells. In addition, we showed that inflammatory cytokines induce translocation of GRP78 from the endoplasmic reticulum to the beta-cell membrane and its subsequent secretion (5,14), providing the ideal environment to become citrullinated in the extracellular space (15). Although it remains unknown which cells are responsible for protein citrullination in the pancreas, PAD2 is highly expressed in NOD islets relative to C57Bl/6 islets (5,16). Also increased levels of PAD4 in neutrophils of type 1 diabetes individuals have been reported (17,18). Interestingly, PAD4 is crucial for the formation of neutrophil extracellular traps (NETs) (19), a process associated with the pathogenesis of type 1 diabetes (20,21). Neutrophils are the first immune cells to infiltrate the islets of NOD mice (20) and have been found in the human pancreas prior to disease onset (21), with a substantial fraction forming NETs (21). Moreover, different studies targeting neutrophil activity or NETs showed a marked protection against diabetes development in NOD mice (20,22–24).

Citrullination does not occur exclusively in type 1 diabetes. In other autoimmune diseases, citrullinated proteins are present in inflamed target tissues and are associated with the break in immune tolerance (25). In rheumatoid arthritis, for example, citrullinated autoantigens are known to be causative (25). Several studies have reported improved disease outcome without any signs of *in vivo* toxicity (26–30) using pan-PAD inhibitors, such as Cl-amidine or BB-Cl-amidine, in animal models for rheumatoid arthritis (26,31,32), multiple sclerosis (33), systemic lupus erythematosus (30,34) and ulcerative colitis (27–29). Disease improvement, through direct inhibition of citrullination, was shown to be linked to decreased NET formation (NETosis) (34–37), modulation of dendritic cell function (37) and a shift in Th1/Th2 profiles (31). Based on these results, PAD inhibition is gaining interest as a strategy to treat or prevent autoimmune diseases that are associated with abnormal PAD activity.

The mechanism by which BB-Cl-amidine and its mother compound Cl-amidine inactivates PAD has been well described (38). Both compounds irreversibly inactivate PAD enzymes through covalent modification of a conserved cysteine in the active site of the PAD enzymes, thereby having an effect on all PAD enzymes. When PAD enzymes become activated they undergo a calcium-dependent conformational change that moves a nucleophilic cysteine residue into the active site and, only then, this cysteine is available for the PAD inhibitor (38). Compared to Cl-amidine, BB-Cl-amidine has a longer *in vivo* half-life (1.75 h vs. ~15 min), a higher cellular potency (EC50 of 8.8±0.6 μM vs >200 μM for Cl-amidine) and a comparable selectivity for the different PAD enzymes (34). With no reports on the potential efficacy of PAD inhibition in type 1 diabetes models, we here evaluated the effect of BB-Cl-amidine in NOD mice. We observed full protection against diabetes development, associated with a decrease in citrullination and in autoantibody titers against citrullinated GRP78. Effects on innate and adaptive immune responses were also observed, with decreased NETosis of bone marrow-derived neutrophils, increased serum Th2 cytokines and regulatory T cells (T_{reg}) in

peripheral tissues, and a decrease in effector memory $CD4^+$ T cells (T_{EM}) and IFNγ-producing $CD4^+$ and $CD8^+$ T cells in the pancreas. These findings point to a role for dysregulated PAD activity and citrullination in autoimmune diabetes and provide initial insight into PAD inhibition as a potential therapeutic strategy.

Research Design and Methods

Mice and treatment regimen

Non-obese diabetic (NOD) mice were inbred and housed under semi-barrier conditions in our animal facility. Eight-week-old female NOD mice were used. Treatments involved subcutaneous injections with BB-Cl-amidine (1µg/g body weight) or vehicle (25% DMSO in PBS) six times per week until 25 weeks of age for diabetes incidence, or until 13 weeks of age for mechanistic studies (29,31,34,39). Experiments were approved by the Institutional Animal Ethics Committee of KULeuven.

Dispersion of murine islets and sorting

Islets were isolated from 10-week-old NOD mice using collagenase (40). After overnight resting, the islets were dispersed into single-cell suspensions by incubation for 90sec at 37°C in 0.025% trypsin-EDTA (Thermo Fisher). Cells were surface stained for cell sorting by flow cytometry as described (40). A detailed protocol is provided in Supplementary data.

RNA isolation, cDNA synthesis and qPCR

RNA isolation and cDNA generation was performed as previously described (40). SYBR green qPCR was performed on a QuantStudio 3 (Thermo Fisher) per manufacturer's instructions. Gene expression levels *of insulin 1 (Ins1), glucagon (Glc*), CD45, *Padi2* and *Padi4* were normalized to the geometrical mean of 3 housekeeping genes (actin, RPL27 and HPRT) and analyzed by relative quantification using the 2^-ΔCt method.

Immunohistochemistry

Five-µm sections of paraffin embedded pancreata were collected at 50µm intervals. Heat-mediated antigen retrieval was performed on deparaffinized sections using citrate buffer (pH6.1; 20min, Dako). To detect citrullination, endogenous peroxidase activity was blocked with 0.5% H_2O_2 in methanol for 20min. Sections were incubated with rabbit anti-citrulline (1:50, Abcam) for 1h and with anti-rabbit HRP Envision (Dako) for 30min. Sections were incubated with DAB (Dako), counterstained with haematoxylin (2min), dehydrated and mounted with DEPEX. For insulin detection, sections were blocked with 10% normal goat serum (Dako) for 20min and incubated with guinea pig anti-insulin (1:150, Dako) for 1h and Alexa Fluor®633-conjugated goat anti-guinea pig (1:500, Life) for 30min. Sections were counterstained with Hoechst (1:2000, Thermo Fisher) and mounted with Mowiol (Polysciences). All incubations were done at room temperature (RT). Imaging was performed using an Olympus BX41 or Zeiss LSM 780 confocal NLO microscope.

Diabetes incidence

Mice were tested for clinical signs of diabetes by evaluating glucose levels in the urine with Diastix Reagent Strips (Bayer). As soon as glucosuria was measured, further follow-up was done by measuring blood glucose levels. Mice were considered diabetic when glucosuria was present and blood glucose levels were higher than 200mg/dL for two consecutive days.

Insulitis

At least 25 islets per mouse were scored for lymphocytic infiltration in a blinded manner using hematoxylin-eosin stained sections.

Insulin content

Pancreata were homogenized in acidic ethanol (91% ethanol, 9% 1M H_3PO_4) at 4°C overnight and sonicated. Insulin content was determined in the supernatant by ELISA (Mercodia) and normalized to the weight of the pancreas.

SDS-PAGE and Western blotting

Protein samples (50µg) were separated on 4-12% Bis-Tris gels (Invitrogen) and blotted onto PVDF membranes (Hybond-ECL, GE Healthcare). To detect citrullination, the anti-modified citrulline Kit (Millipore) was used. Membranes were incubated with SuperSignal™ West Femto Maximum Sensitivity Substrate (Thermo Fisher) and revealed using the ImageQuant LAS 500 system (GE Healthcare). Blots were normalized by re-probing for GAPDH (Thermo Fisher).

Proteomic analysis making use of biotin-phenylglyoxal labeling

DMSO (n=4) and BB-Cl-amidine treated (n=4) mice pancreata were pooled in buffer (50mM HEPES pH 7.6, 0.5% NP40 and 1mM PMSF) and homogenized using a tissue homogenizer (maximum speed, 3x20sec at 10min intervals). The lysed tissue samples were centrifuged (12,000 rpm, 30min) at 4°C. The supernatants were isolated, and the protein concentration was determined using the DC™ (detergent compatible) assay. Equal protein concentrations from DMSO and BB-Cl-amidine treated samples were labeled with biotin-phenylglyoxal (biotin-PG) in quadruplicate as previously described (41). A detailed protocol is provided in Supplementary data.

TMT labeling and LC-MS/MS analysis

A total of eight peptide digests were obtained from quadruplicate biotin-PG labeling of the DMSO and BB-Cl-amidine treated samples. The samples were labeled using a TMT labeling

system and prepared for LC-MS/MS analysis on a NanoAcquity UPLC (Waters Corporation) coupled to an Orbitrap Fusion Lumos Tribrid (Thermo Fisher) mass spectrometer. The raw data were processed using Proteome Discoverer (Thermo Fisher, version 2.1.1.21) and searched against SwissProt murine (downloaded 07/2019) database using Mascot (Matrix Science, version 2.6.2). A detailed protocol is provided in Supplementary data.

Autoantibody assays

Mouse serum autoantibody levels against citrullinated GRP78 were determined by an in-house developed MesoScale Discovery (MSD) ELISA. *In vitro* citrullinated GRP78 (IVC GRP78) was generated as described (5). Multi-array 96 plates (MSD) were coated (overnight, 4°C) with 5µg/mL IVC GRP78 in PBS (pH 7) or with 3% skimmed milk in PBS (uncoated control). Blocking was performed with 3% skimmed milk in PBS with 0.5% Tween 20 (2h at RT). Mouse serum was diluted 1:5 in blocking solution and incubated for 2h at RT. Wells were incubated for 2h at RT with SULFO-TAG labeled goat anti-mouse IgG. Read buffer was added and detection was done on an MSD reader. To exclude nonspecific signals, each sample had its background signal (serum binding in uncoated well) subtracted from the reading.

NETosis

Bone marrow-derived cells were harvested from the humeri, tibias and femurs and neutrophils were isolated using the Neutrophil Isolation Kit (Miltenyi). Neutrophils were cultured on coverslips, pre-coated with 0.01% Poly L-lysine (Sigma), for 3h at 37°C in 5% CO_2. Paraformaldehyde-fixed neutrophils were stained with Hoechst (Thermo Fisher) and NETosis was quantified blindly using a Nikon Eclipse TI microscope. Percentage of NET releasing cells was calculated by normalizing to the total amount of cells. Images were taken on a Zeiss LSM 880 confocal Airyscan microscope.

Cytokine measurement in serum

Serum levels of IFNγ, IL-4 and IL-10 were determined using a V-plex assay from MSD, by a single measurement. All concentrations were above the lower limit of detection (LLOD).

Immune cell phenotyping

Blood was incubated 3 times with NH_4Cl to lyse red blood cells. Single cell suspensions from spleen were obtained by mechanical disruption, while the pancreas was enzymatically digested for 15min at 37°C in RPMI (72400, Thermo Fisher) supplemented with 5% bovine serum, 0.05mM beta-mercaptoethanol, 100U/mL penicillin, 100U/mL streptomycin, 1mg/mL collagenase VII and 0.02mg/mL DNase I. For phenotypic characterization of T_{reg}, T_{EM}, central memory (T_{CM}) and naïve ($T_{naïve}$) T-cell subsets, cell suspensions were stained with Zombie Yellow Fixable Viability dye (Biolegend) and with antibodies against CD4 (BD), CD3, CD8, CD44, CD62L, CD25 and Foxp3 (eBioscience). Intracellular staining was performed with Foxp3/Transcriptional Factor Staining Buffer Set (eBioscience). To evaluate the effect of BB-Cl-amidine treatment on cytokine production, 5 x 10^5 cells from the spleen and pancreas were stimulated *in vitro* with 0.025µg/mL phorbol-12-myristate-13-acetate (PMA) (Sigma) and 0.25µg/mL ionomycin (Sigma) in the presence of GolgiStop (1:500, BD) for 4h at 37°C in 5% CO_2. Next, cells were incubated with antibodies against CD4 and CD8, treated with Cytofix/Cytoperm (BD), and stained with anti-IFNγ antibody (eBioscience). Samples were acquired on a BD FACS Canto II and analyzed with FlowJo software (TreeStar). The percentage of cytokine-producing cells was determined and the expression level of the cytokine was assessed using geometric mean fluorescence intensity (MFI). For each

experiment, the geometric MFI of each sample was normalized to the average geometric MFI of the DMSO group (MFI fold change).

Statistics

Data were analyzed using GraphPad Prism 8 or Scaffold software. Diabetes incidence was evaluated by Kaplan-Meier survival analysis with Mantel-Cox log-rank test. Data were expressed as mean ± SEM and, after exclusion of outliers, data were analyzed by one-way ANOVA, unpaired t-test with Welch's correction, or Mann-Whitney U test, as indicated. $P<0.05$ was considered statistically significant.

Data and Resource Availability

All datasets generated during the current study are available from the corresponding author upon request.

Results

Pancreatic islets express *Padi2* both in endocrine and in infiltrating immune cells

Although we have previously shown that islets of 3- and 10-week-old NOD mice have elevated PAD activity levels and enhanced *Padi2* mRNA expression compared to C57Bl/6 islets (5), it remains to be elucidated which cell population within the islets is responsible for this high PAD activity. To investigate this, we performed flow cytometry sorting on 10-week-old NOD islet cells making use of an antibody panel consisting of CD71, CD24, CD49f and CD45 to enable isolation of highly purified alpha- and beta-cells (40), as well as immune cells. The purity of immune cell fraction was confirmed by marginal expression of *insulin 1 (ins1)* and *glucagon (glc*). Purity of alpha- and beta-cell fractions was confirmed by complete absence of leukocyte marker *CD45* in both fractions, and marginal expression levels of *glc* (in beta-cells) and *ins1* (in alpha-cells) (Fig. 1A-C). In immune, as well as in alpha- and beta-cells, *Padi2* was clearly expressed (Fig.1D), with a trend to higher levels in immune and beta-cells, as compared to alpha-cells. Of note, *Padi4* mRNA levels were below the detection limit (data not shown). In line with this, immunohistochemical analysis of citrullination in pancreas sections of NOD mice demonstrated intense staining in infiltrated immune cells, while endocrine islet cells stained weakly positive. Parallel staining in age-matched C57Bl/6, also showed citrullination in the endocrine islet cells (Fig. 1E and Suppl. Fig. 1). These results indicate that citrullination occurs in immune cells infiltrated in the islets and, also in endocrine alpha- and beta-cells even in non-pathological conditions.

BB-Cl-amidine treatment prevents diabetes development in NOD mice and preserves insulin production

To examine the role of citrullination on diabetes development, NOD mice were treated with BB-Cl-amidine. Treatment was started at 8 weeks of age, a time point at which insulitis is already ongoing in NOD mice. BB-Cl-amidine treatment fully prevented diabetes development, with all mice free of diabetes until 25 weeks of age, against 44% diabetes-free in DMSO treated mice ($P<0.001$; Fig. 2A). Therapy was well tolerated as confirmed by normal weight curves (Suppl. Fig. 2). Evaluation of pancreatic insulin content at 13 weeks of age, before the onset of diabetes, showed a 4-fold increase of insulin in the pancreas of BB-Cl-amidine treated mice compared to the control ($P<0.01$; Fig. 2B and C), pointing to preserved insulin production in BB-Cl-amidine treated mice.

BB-Cl-amidine treatment reduces citrullination in the pancreas and autoantibody formation against citrullinated GRP78

To evaluate the direct effect of BB-Cl-amidine on inhibition of citrullination, we performed immunohistochemical staining of citrullinated protein residues on pancreatic sections, showing a reduced staining intensity in BB-Cl-amidine treated compared to DMSO treated mice (Fig. 3A and Suppl. Fig. 3). Quantification of the overall level of citrullinated proteins in the pancreas of BB-Cl-amidine and vehicle-treated NOD mice by Western blotting demonstrated that PAD inhibition reduced the total level of protein citrullination by about 50% ($P<0.01$; Fig. 3B and C). This finding was further confirmed and extended by more quantitative LC-MS/MS analysis. A total of 1,003 citrullinated proteins were identified in pancreata from BB-Cl-amidine and vehicle treated mice, of which 765 were significantly decreased in abundance by

the treatment regimen (Fig. 3D and Suppl. Table 1 and 2). Interestingly, citrullinated GRP78, reported by our group as an autoantigen in murine and human type 1 diabetes (5,10), was the most significantly reduced citrullinated protein, with a decrease of 2.66-fold ($P<0.0001$). We have previously reported the generation of autoantibodies against citrullinated GRP78 in NOD mice (5). In line with this, we observed here that BB-Cl-amidine treatment decreased autoantibody titers against citrullinated GRP78, both at 13 ($P<0.05$; Fig. 3E) and 25 weeks of age ($P<0.05$; Fig. 3F).

BB-Cl-amidine treatment decreases spontaneous NET formation in bone marrow-derived neutrophils

Neutrophils have been suggested to play an important role in the pathogenesis of autoimmune diabetes, as they are the first immune cells to infiltrate the islets of NOD mice (20). Also in type 1 diabetes patients, neutrophil infiltration is observed in the pancreas, even prior to disease onset, with some degree of NETosis (21). Since citrullination is a prerequisite for the initiation of NETosis, we questioned here if BB-Cl-amidine treatment could have an impact on the propensity of neutrophils to form NETs. To this end, spontaneous NETosis was assessed in bone marrow-derived neutrophils isolated from BB-Cl-amidine or vehicle-treated mice. NETosis was significantly reduced in neutrophils from mice treated with BB-Cl-amidine ($P<0.05$; Fig. 4). This finding shows that systemic administration of BB-Cl-amidine has an effect on the capacity of neutrophils to form NETs.

BB-Cl-amidine alters the phenotype and cytokine production of immune infiltrate in the islets

The finding of preserved insulin production by BB-Cl-amidine tempted us to investigate the degree and phenotype of immune infiltration. To this end, immunohistochemical evaluation of islet immune infiltration at 13 weeks of age showed only a moderate overall decrease of insulitis in the BB-Cl-amidine group (Fig. 5A), suggesting a less destructive form of insulitis. To evaluate this further, we measured *in vitro* cytokine production of the immune cells isolated from the pancreas. Although the overall frequency of IFNγ-producing T cells was low in both groups, mice treated with BB-Cl-amidine presented a significantly lower percentage of IFNγ-producing $CD4^+$ and $CD8^+$ T cells ($P<0.01$ and $P<0.05$ respectively; Fig. 5B and C). Evaluating the phenotype of immune cells in the pancreas (representative gating strategy in Suppl. Fig. 4A), revealed a significant decrease in the percentage of $CD4^+$ T_{EM} cells ($P<0.05$; Fig. 5E) in BB-Cl-amidine treated mice, whereas no changes were observed in the frequency of T_{reg} (Fig. 5D). No differences were observed in $CD4^+$ and $CD8^+$ $T_{naïve}$ and T_{CM} subsets (Suppl. Fig. 5). Collectively, these data indicate that, although only a minor change in the overall level of insulitis, BB-Cl-amidine alters the phenotype of infiltrating immune cells, as demonstrated by the decrease in Th1 cytokine production and reduction of T_{EM} cells locally in the pancreas.

BB-Cl-amidine treatment is associated with a Th1 to Th2 serum cytokine shift, and of T_{EM} to Treg in the periphery

Next, we sought to investigate the effect of BB-Cl-amidine treatment on Th1 and Th2 profiles and immune cell phenotype in the periphery, as BB-Cl-amidine has been shown to act through this pathway in other disease models (31). First, we measured serum levels of Th1 and Th2 cytokines in BB-Cl-amidine or vehicle-treated NOD mice. Whereas no significant changes were measured in circulating IFNγ titers (Fig. 6A), IL-4 and IL-10 titers were significantly increased in the BB-Cl-amidine treated group ($P<0.01$ for both; Fig. 6B and C). This resulted in an overall reduction in the IFNγ/IL-10 ratio ($P<0.05$; Fig. 6D) (42). In the spleen of BB-Cl-

amidine treated mice, there was a decrease in IFNγ production indicated by the reduced frequency of IFNγ-producing $CD4^+$ T cells ($P<0.01$; Fig. 6E), as well as the lower expression of IFNγ in IFNγ-producing $CD4^+$ and $CD8^+$ T-cell populations ($P<0.0001$ for both; Fig. 6F and H). To specifically investigate the effect on the cellular phenotype of immune cell subsets, we used flow cytometry to study T-cell subsets in the blood and spleen (representative gating strategy in Suppl. Fig. 4B and C). This revealed that BB-Cl-amidine induced a significant increase in the percentage of T_{reg} in blood ($P<0.05$; Fig. 7A) and spleen ($P<0.01$; Fig. 7D). Regarding T_{EM} ($CD4^+$ and $CD8^+$) in the periphery, there was a significant decrease in the percentage of $CD4^+$ T_{EM} cells in the blood and of splenic $CD8^+$ T_{EM} cells ($P<0.05$ and $P<0.001$, respectively; Fig. 7B and F). No changes were observed in $CD4^+$ and $CD8^+$ T_{CM} populations in the blood and spleen, whereas $CD4^+$ and $CD8^+$ $T_{naïve}$ in blood (both $P<0.05$; Suppl. Fig. 6A and C) and $CD8^+$ $T_{naïve}$ in spleen ($P<0.01$; Suppl. Fig. 6G) were increased in BB-Cl-amidine treated mice. These findings suggest that in the periphery, BB-Cl-amidine induces a shift towards Th2 cytokine production, a decrease in T_{EM} cells and an induction of T_{reg} cells.

Discussion

This study describes the effect of the pan-PAD inhibitor BB-Cl-amidine, showing a complete prevention of diabetes development in NOD mice. This finding highlights the involvement of inflammation-induced citrullination in diabetes development and adds type 1 diabetes to the list of autoimmune diseases in which citrullination participates in disease pathogenesis, a list that includes rheumatoid arthritis (26,31,32), multiple sclerosis (33), lupus (30,34) and ulcerative colitis (27–29). This observation may have significant implications for the development of new therapeutic strategies to mitigate the progression and/or development of type 1 diabetes.

We here provide evidence that the previously reported high expression of *Padi2* in islets of NOD mice (5,16) originates from both the endocrine cells, including alpha- and beta-cells, as well as from the infiltrating immune cells, thereby conclusively demonstrating that beta-cells themselves have the capacity to citrullinate. This finding formed the basis for evaluating the effect of PAD inhibition in NOD mice. In the current treatment regimen, we started treatment at 8 weeks of age, a time point at which insulitis is already ongoing. The observation that inhibition of PAD activity, and thus citrullination, protected NOD mice against diabetes development suggests that citrullination may play a role in the amplification of the disease rather than being an initial trigger in breaking of immune tolerance. This strengthens our earlier findings of minor autoreactivity against citrullinated GRP78 in prediabetic NOD mice (5) and the increased occurrence of autoantibodies and autoreactive T-cell responses in long-standing T1D patients versus new onset patients (10). This view also fits well with the knowledge that citrullination is mostly associated with inflammation, thereby playing a role in several autoimmune diseases, where citrullination takes place in the inflamed target tissues (26–34). The low levels of citrullination in islets of C57Bl/6 mice further demonstrate that citrullination

is present already under physiological conditions, however, the degree of citrullination is markedly increased in NOD islets associated with immune infiltration.

BB-Cl-amidine treatment is effective in decreasing overall levels of citrullination in the pancreas, as shown by Western blotting and quantitative LC-MS/MS. Of interest, the most significant reduction was measured for citrullinated GRP78. In line with this, the level of autoantibodies against citrullinated GRP78 is decreased in the circulation of BB-Cl-amidine treated NOD mice. Although autoantibodies are not thought to be pathogenic in type 1 diabetes, this finding underlines the important effect of BB-Cl-amidine on reducing the antigenicity of beta-cell proteins in the inflamed islet environment.

Pan-PAD inhibitors are known to alter NET release (34–37). Neutrophils and NETosis are thought to play an important role in the initiation and perpetuation of type 1 diabetes (20,21,43). Here, we show that BB-Cl-amidine reduces spontaneous NET release *ex vivo* from bone marrow-derived neutrophils of NOD mice, a finding that may be linked to a decrease in citrullinated histone H3 levels. Indeed, citrullination of histone H3, mediated by activation of PADs in neutrophils, is an initiating factor for the formation of NETs (44), and has been shown to be reduced by PAD inhibition (36). Our results are in line with studies in lupus (30,34) and collagen-induced arthritis (37), demonstrating that reduced NETosis in response to PAD inhibition is associated with disease amelioration.

Looking at the islet level, BB-Cl-amidine treatment resulted in only a marginal reduction of insulitis, whereas pancreatic insulin levels were preserved. However, we did observe a significant reduction in the percentage of $CD4^+$ T_{EM} cells and in the frequency of IFNγ-producing $CD4^+$ and $CD8^+$ T cells in the pancreas of BB-Cl-amidine treated mice. The observed reduction in IFNγ production may reflect an impaired effector function of the infiltrating immune cells (45). These results suggest that the immune cell infiltrate in BB-Cl-amidine treated mice is less aggressive (46).

Our results on increased frequency of T_{reg} in the blood and spleen demonstrate a peripheral effect of BB-Cl-amidine. Additionally, splenic IFNγ production of BB-Cl-amidine treated mice was significantly reduced. These results suggest a more regulatory environment that favors immune tolerance and prevents intensification of the immune assault. Also, with Th1/Th2 polarization thought to play a role in T1D pathogenesis, the significant increase in IL-4 and decrease in the IFNγ/IL-10 ratio in the circulation of BB-Cl-amidine treated mice supports this hypothesis. Of note, whether Th1/Th2 polarization is a cause rather than a consequence of disease development, is not fully established. In line with these findings, an induction of Th2 cells by BB-Cl-amidine has been shown in a mouse model of rheumatoid arthritis (31) and a direct effect of BB-Cl-amidine on enhancing the differentiation of Th2 subsets through inhibition of GATA3 citrullination was demonstrated mechanistically by Sun *et al.* (47).

For the first time, a pan-PAD inhibitor was used in a very long treatment regimen (17 weeks), with no detrimental side effects observed. This, together with reported disease amelioration with the use of PAD inhibitors in other autoimmune models, opens the road to potential clinical therapeutic applications. However, since PADs also participate in physiological processes (11), such as gene regulation and nerve myelination, such therapeutic treatment regimens will need careful consideration. The recent development of specific PAD2 (48) and PAD4 (49) inhibitors, as well as reversible PAD inhibitors (50), may be a solution, but their efficacy to treat autoimmune diseases remains to be confirmed. Results from ongoing studies may further invite to consider PAD inhibition as a therapeutic strategy, not only for type 1 diabetes but also for other autoimmune diseases.

In conclusion, treatment of NOD mice with BB-Cl-amidine resulted in complete diabetes prevention, associated with decreased protein citrullination, anti-citrulline autoantibody formation, NETosis, and *in situ* IFNγ responses. We postulate that these effects, combined with

the direct effect of PAD inhibition on T cells, might lead to a less aggressive inflammatory environment in the islets and in the periphery. Our findings align with previous reports that citrullination plays a pathogenic role in type 1 diabetes and demonstrate that PAD inhibition is an attractive target for clinical therapeutic applications in autoimmunity.

Acknowledgements. The technical assistance of Eline Desager, Jos Laureys, Marijke Viaene and Martine Gilis (Laboratory of Clinical and Experimental Endocrinology, KU Leuven) is greatly appreciated. We thank the KU Leuven Flow Cytometry Core Facility for assistance with flow cytometry. Fluorescent images were recorded on a Zeiss LSM 780 – SP Mai Tai HP DS (Cell and Tissue Imaging Cluster (CIC), supported by Hercules AKUL/11/37 and FWO G.0929.15 to Pieter Vanden Berghe, University of Leuven) or on a Zeiss LSM 880 – Airyscan (Cell and Tissue Imaging Cluster (CIC), supported by Hercules AKUL/15/37_GOH1816N and FWO G.0929.15 to Pieter Vanden Berghe, University of Leuven). We thank UMass Medical School proteomics core facility director Dr. Scott Shaffer for helping with proteomics analysis and Dr. Roshanak Aslebagh for running proteomics samples.

Funding. This work was supported by IMI2-JU under grant agreement No 115797 (INNODIA) and No 945268 (INNODIA HARVEST). This Joint Undertaking receives support from the Union's Horizon 2020 research and innovation program and "EFPIA", 'JDRF" and "The Leona M. and Harry B. Helmsley Charitable Trust". Further support came from the KU Leuven (C16/18/006), the Flemish Research Foundation (a predoctoral fellowship for SB (11A0220N), DPC (11Y6716N) and AC (1189518N) and a post-doctoral fellowship for MB (12R0719N)), and the NIH (R35GM118112 to PRT).

Duality of interest. No potential conflicts of interest relevant to this article are to be reported.

Author Contributions. FMCS performed design, conduction, analysis and interpretation of the data and wrote and edited the manuscript. SB helped with the design of the NETosis data, besides conducting and analyzing them. YB contributed by injecting mice and performing experiments. RT and PRT conducted and analyzed the proteomic analysis of the biotin-PG labeled samples and the LC-MS/MS. DPC helped with mice treatment and contributed to the design and analysis of the FACS data. CB and RS performed and analyzed the islets isolation, sorting and qPCR. AC helped with conduction of experiments. SY and RM contributed to the design and interpretation of islet experiments. SM and PRT provided the BB-Cl-amidine. CM, LO and MB designed research, interpreted data and wrote and edited the manuscript. MB also conducted and analyzed experiments. All authors edited the manuscript and gave their final approval of the version to be published. CM and LO are the guarantors of this work and, as such, had full access to all the data in the study and take responsibility for the integrity of the data and the accuracy of the data analysis.

Prior Presentation. This study has not been presented before.

References

1. Mannering SI, Harrison LC, Williamson NA, Morris JS, Thearle DJ, Jensen KP, et al. The insulin A-chain epitope recognized by human T cells is posttranslationally modified. J Exp Med. 2005;202(9):1191–7.
2. Delong T, Baker RL, He J, Barbour G, Bradley B, Haskins K. Diabetogenic T-cell clones recognize an altered peptide of chromogranin A. Diabetes. 2012;61(12):3239–46.
3. Van Lummel M, Duinkerken G, Van Veelen PA, De Ru A, Cordfunke R, Zaldumbide A, et al. Posttranslational modification of HLA-DQ binding islet autoantigens in type 1 diabetes. Diabetes. 2014;63(1):237–47.
4. McGinty JW, Chow IT, Greenbaum C, Odegard J, Kwok WW, James EA. Recognition of posttranslationally modified GAD65 epitopes in subjects with type 1 diabetes. Diabetes. 2014;63(9):3033–40.
5. Rondas D, Crèvecoeur I, D'Hertog W, Ferreira GB, Staes A, Garg AD, et al. Citrullinated glucose-regulated protein 78 is an autoantigen in type 1 diabetes. Diabetes. 2015;64(2):573–86.
6. Babon JAB, Denicola ME, Blodgett DM, Crèvecoeur I, Buttrick TS, Maehr R, et al. Analysis of self-antigen specificity of islet-infiltrating T cells from human donors with type 1 diabetes. Nat Med. 2016;22(12):1482–7.
7. Strollo R, Vinci C, Napoli N, Pozzilli P, Ludvigsson J, Nissim A. Antibodies to post-translationally modified insulin as a novel biomarker for prediction of type 1 diabetes in children. Diabetologia. 2017;60(8):1467–74.
8. Marre ML, Mcginty JW, Chow I, Denicola ME, Beck NW, Kent SC, et al. Modifying Enzymes Are Elicited by ER Stress , Generating Epitopes That Are Selectively Recognized by CD4 + T Cells in Patients With Type 1 Diabetes. Diabetes. 2018;67(July):1356–68.
9. Gonzalez-Duque S, Azoury ME, Colli ML, Afonso G, Turatsinze JV, Nigi L, et al. Conventional and Neo-antigenic Peptides Presented by β Cells Are Targeted by Circulating Naïve CD8+ T Cells in Type 1 Diabetic and Healthy Donors. Cell Metab. 2018;28(6):946-960.e6.
10. Buitinga M, Callebaut A, Marques Câmara Sodré F, Crèvecoeur I, Blahnik-Fagan G, Yang M, et al. Inflammation-Induced Citrullinated Glucose-Regulated Protein 78 Elicits Immune Responses in Human Type 1 Diabetes. Diabetes. 2018;67(11):2337–48.
11. Witalison EE, Thompson PR, Hofseth LJ. Protein Arginine Deiminases and Associated Cirtullination: Physiological Functions and Diseases Associated with Dysregulation. Curr Drug Targets. 2015;16(7):700–710.
12. Nguyen H, James EA. Immune recognition of citrullinated epitopes. Immunology. 2016;149(2):131–8.
13. McGinty JW, Marré ML, Bajzik V, Piganelli JD, James EA. T Cell Epitopes and Post-Translationally Modified Epitopes in Type 1 Diabetes. Vol. 15, Current Diabetes Reports. 2015. p. 1–14.
14. Vig S, Buitinga M, Rondas D, Crèvecoeur I, van Zandvoort M, Waelkens E, et al. Cytokine-induced translocation of GRP78 to the plasma membrane triggers a pro-apoptotic feedback loop in pancreatic beta cells. Cell Death Dis [Internet]. 2019;10(4). Available from: http://dx.doi.org/10.1038/s41419-019-1518-0
15. Zhou Y, Chen B, Mittereder N, Chaerkady R, Strain M, An LL, et al. Spontaneous secretion of the citrullination enzyme PAD2 and cell surface exposure of PAD4 by neutrophils. Front Immunol. 2017;8(SEP):1–16.

16. Crèvecoeur I, Gudmundsdottir V, Vig S, Marques Câmara Sodré F, D'Hertog W, Fierro AC, et al. Early differences in islets from prediabetic NOD mice: combined microarray and proteomic analysis. Diabetologia. 2017;60(3):475–89.
17. Wong SL, Demers M, Martinod K, Gallant M, Wang Y, Goldfine AB, et al. Diabetes primes neutrophils to undergo NETosis, which impairs wound healing. Nat Med. 2015;21(7):815–9.
18. You Q, He DM, Shu GF, Cao B, Xia YQ, Xing Y, et al. Increased formation of neutrophil extracellular traps is associated with gut leakage in patients with type 1 but not type 2 diabetes. J Diabetes. 2019;11(8):665–73.
19. Wang Y, Li M, Stadler S, Correll S, Li P, Wang D, et al. Histone hypercitrullination mediates chromatin decondensation and neutrophil extracellular trap formation. J Cell Biol. 2009;184(2):205–13.
20. Diana J, Simoni Y, Furio L, Beaudoin L, Agerberth B, Barrat F, et al. Crosstalk between neutrophils, B-1a cells and plasmacytoid dendritic cells initiates autoimmune diabetes. Nat Med. 2013;19(1):65–73.
21. Vecchio F, Buono N Lo, Stabilini A, Nigi L, Dufort MJ, Geyer S, et al. Abnormal neutrophil signature in the blood and pancreas of presymptomatic and symptomatic type 1 diabetes. JCI Insight [Internet]. 2018;3(18):1–17. Available from: https://insight.jci.org/articles/view/122146
22. Citro A, Valle A, Cantarelli E, Mercalli A, Pellegrini S, Liberati D, et al. CXCR1/2 inhibition blocks and reverses type 1 diabetes in mice. Diabetes. 2015;64(4):1329–40.
23. Liang Y, Wang X, He D, You Q, Zhang T, Dong W, et al. Ameliorating gut microenvironment through staphylococcal nuclease-mediated intestinal NETs degradation for prevention of type 1 diabetes in NOD mice. Life Sci [Internet]. 2019;221(February):301–10. Available from: https://doi.org/10.1016/j.lfs.2019.02.034
24. Shu L, Zhong L, Xiao Y, Wu X, Liu Y, Jiang X, et al. Neutrophil elastase triggers the development of autoimmune diabetes by exacerbating innate immune responses in pancreatic islets of non-obese diabetic mice. Clin Sci (Lond). 2020;134(13):1679–96.
25. Alghamdi M, Alasmari D, Assiri A, Mattar E, Aljaddawi AA, Alattas SG, et al. An overview of the intrinsic role of citrullination in autoimmune disorders. J Immunol Res. 2019;2019.
26. Kawaguchi H, Matsumoto I, Osada A, Kurata I, Ebe H, Tanaka Y, et al. Peptidyl arginine deiminase inhibition suppresses arthritis via decreased protein citrullination in joints and serum with the downregulation of interleukin-6. Mod Rheumatol [Internet]. 2019;29(6):964–9. Available from: https://doi.org/10.1080/14397595.2018.1532545
27. Chumanevich AA, Causey CP, Knuckley BA, Jones JE, Poudyal D, Chumanevich AP, et al. Suppression of colitis in mice by Cl-amidine: A novel peptidylarginine deiminase inhibitor. Am J Physiol - Gastrointest Liver Physiol. 2011;300(6):929–38.
28. Witalison EE, Cui X, Causey CP, Thompson PR, Hofseth LJ. Molecular targeting of protein arginine deiminases to suppress colitis and prevent colon cancer. Oncotarget. 2015;6(34):36053–62.
29. Chumanevich AA, Chaparala A, Witalison EE, Tashkandi H, Hofseth AB, Lane C, et al. Looking for the best anti-colitis medicine: A comparative analysis of current and prospective compounds. Oncotarget. 2017;8(1):228–37.
30. Knight JS, Zhao W, Luo W, Subramanian V, Dell AAO, Yalavarthi S, et al. Peptidylarginine deiminase inhibition is immunomodulatory and vasculoprotective in murine lupus. J Clin Invest [Internet]. 2013;123(7):2981–93. Available from:

https://www.jci.org/articles/view/67390?trendmd-shared=%25SPONSORED%25
31. Kawalkowska J, Quirke AM, Ghari F, Davis S, Subramanian V, Thompson PR, et al. Abrogation of collagen-induced arthritis by a peptidyl arginine deiminase inhibitor is associated with modulation of T cell-mediated immune responses. Sci Rep [Internet]. 2016;6(February):1–12. Available from: http://dx.doi.org/10.1038/srep26430
32. Willis VC, Gizinski AM, Banda NK, Causey CP, Knuckley B, Cordova KN, et al. N-α-Benzoyl-N5-(2-Chloro-1-Iminoethyl)-l-Ornithine Amide, a Protein Arginine Deiminase Inhibitor, Reduces the Severity of Murine Collagen-Induced Arthritis. J Immunol. 2011;186(7):4396–404.
33. Moscarello MA, Lei H, Mastronardi FG, Winer S, Tsui H, Li Z, et al. Inhibition of peptidyl-arginine deiminases reverses protein-hypercitrullination and disease in mouse models of multiple sclerosis. DMM Dis Model Mech. 2013;6(2):467–78.
34. Knight JS, Subramanian V, O'Dell AA, Yalavarthi S, Zhao W, Smith CK, et al. Peptidylarginine deiminase inhibition disrupts NET formation and protects against kidney, skin and vascular disease in lupus-prone MRL/ lpr mice. Ann Rheum Dis. 2015;74(12):2199–206.
35. Madhi R, Rahman M, Taha D, Mörgelin M, Thorlacius H. Targeting peptidylarginine deiminase reduces neutrophil extracellular trap formation and tissue injury in severe acute pancreatitis. J Cell Physiol. 2019;234(7):11850–60.
36. Biron BM, Chung C, Brien XMO, Chen Y, Reichner J, Ayala A. Cl-amidine Prevents Histone 3 Citrullination, NET Formation, and Improves Survival in a Murine Sepsis Model. J Innate Immun. 2018;9(1):22–32.
37. Papadaki G, Kambas K, Choulaki C, Vlachou K, Drakos E, Bertsias G, et al. Neutrophil extracellular traps exacerbate Th1-mediated autoimmune responses in rheumatoid arthritis by promoting DC maturation. Eur J Immunol. 2016;46(11):2542–54.
38. Luo Y, Arita K, Bhatia M, Knuckley B, Lee YH, Stallcup MR, et al. Inhibitors and inactivators of protein arginine deiminase 4: Functional and structural characterization. Biochemistry. 2006;45(39):11727–36.
39. Ghari F, Quirke AM, Munro S, Kawalkowska J, Picaud S, McGouran J, et al. Citrullination-acetylation interplay guides E2F-1 activity during the inflammatory response. Sci Adv. 2016;2(2).
40. Berthault C, Staels W, Scharfmann R. Purification of pancreatic endocrine subsets reveals increased iron metabolism in beta-cells. Mol Metab [Internet]. 2020;42(August). Available from: https://doi.org/10.1016/j.molmet.2020.101060
41. Tilvawala R, Nguyen SH, Maurais AJ, Nemmara V V., Nagar M, Salinger AJ, et al. The Rheumatoid Arthritis-Associated Citrullinome. Cell Chem Biol [Internet]. 2018;25(6):691-704.e6. Available from: https://doi.org/10.1016/j.chembiol.2018.03.002
42. Schloot NC, Hanifi-Moghaddam P, Goebel C, Shatavi S V., Flohé S, Kolb H, et al. Serum IFN-γ and IL-10 levels are associated with disease progression in non-obese diabetic mice. Diabetes Metab Res Rev. 2002;18(1):64–70.
43. Valle A, Giamporcaro GM, Scavini M, Stabilini A, Grogan P, Bianconi E, et al. Reduction of circulating neutrophils precedes and accompanies type 1 diabetes. Diabetes. 2013;
44. Jorch SK, Kubes P. An emerging role for neutrophil extracellular traps in noninfectious disease. Nat Med. 2017;23(3):279–87.
45. Bhat P, Leggatt G, Waterhouse N, Frazer IH. Interferon-γ derived from cytotoxic lymphocytes directly enhances their motility and cytotoxicity. Cell Death Dis [Internet].

2017;8(6):e2836. Available from: http://dx.doi.org/10.1038/cddis.2017.67
46. Mallone R, van Endert P. T cells in the pathogenesis of type 1 diabetes. Curr Diab Rep. 2008;8(2):101–6.
47. Sun B, Chang HH, Salinger A, Tomita B, Bawadekar M, Holmes CL, et al. Reciprocal regulation of Th2 and Th17 cells by PAD2-mediated citrullination. JCI Insight. 2019;4(22).
48. Muth A, Subramanian V, Beaumont E, Nagar M, Kerry P, Mcewan P, et al. Development of a Selective Inhibitor of Protein Arginine Deiminase 2. J Med Chem. 2017;60:3198−3211.
49. Lewis HD, Liddle J, Coote JE, Atkinson SJ, Barker MD, Bax BD, et al. Inhibition of PAD4 activity is sufficient to disrupt mouse and human NET formation. Nat Chem Biol. 2015;11.
50. Aliko A, Kamińska M, Falkowski K, Bielecka E, Benedyk-Machaczka M, Malicki S, et al. Discovery of novel potential reversible peptidyl arginine deiminase inhibitor. Int J Mol Sci. 2019;20(9).

Figures legends

Figure 1 - *Padi2* is expressed in immune, alpha- and beta-cells from NOD islets. A-C: mRNA expression level in pancreatic immune cells (Imm), alpha-cells and beta-cells for the leukocyte marker *CD45* (A); alpha-cell marker glucagon (*Glc*) (B); beta-cell marker insulin 1 (*Ins1*) (C); and *Padi2* (D) (n = 3; 3 independent experiments were performed with one mouse per experiment). E: Representative immunohistochemical staining against citrulline in pancreas sections of C57Bl/6 and NOD mice (scale bar = 50µm). All sections where mounted on one slide to enable good comparison. Data in A–D are mean ± SEM and were analyzed by one-way ANOVA. **P<0.01, ***P<0.001 and ****P<0.0001.

Figure 2 - BB-Cl-amidine treatment prevents diabetes development in NOD mice and preserves pancreatic insulin production. A: Percentage of diabetes free NOD mice treated with DMSO or BB-Cl-amidine. Eight-week-old female littermate NOD mice were injected subcutaneously with vehicle (25% DMSO in PBS) or BB-Cl-amidine (1µg/g body weight) six times per week until 25 weeks of age and followed-up for diabetes development (n = 17-18 mice per group; 2 independent cohorts were performed with at least eight mice per group per experiment). B: Pancreatic insulin content of 13-week-old NOD mice treated with DMSO or BB-Cl-amidine from 8-13 weeks of age (n = 8-10; two independent experiments were performed with 4-5 mice per group per experiment). C: Illustrative images of insulin staining in the pancreas of 13-week-old NOD mice treated from 8-13 weeks of age with DMSO or BB-Cl-amidine (scale bar = 50µm). Data in A were evaluated by Kaplan-Meier survival analysis with Mantel-Cox log-rank test. Data in B are mean ± SEM and were analyzed by unpaired t-test with Welch's correction. **P<0.01 and ***P<0.001.

Figure 3 - BB-Cl-amidine treatment reduces citrullination in the pancreas and the formation of circulating autoantibodies. A: Representative immunohistochemical staining against citrulline in pancreas sections of 13-week-old DMSO or BB-Cl-amidine treated NOD mice (scale bar = 50µm). All sections where mounted on one slide to enable good comparison. B: Representative Western blot with anti-modified citrulline antibody in pancreatic lysates of 13-week-old DMSO or BB-Cl-amidine treated NOD mice. C: Optical density ratio (sum of citrullinated bands/GAPDH band) of pancreas samples from DMSO or BB-Cl-amidine treated mice (n = 4 mice per group). D: Volcano plot showing significant fold changes in citrullinated proteins in pancreas of NOD mice treated with BB-Cl-amidine, from 8 until 13 weeks of age, compared to DMSO treated NOD mice. The x axis represents $\log_2$ expression fold changes (BB-Cl-amidine/DMSO), and the y axis represents the adjusted p-values (as $-\log_{10}$). E-F: Comparison between the serum levels of anti-citrullinated GRP78 antibodies in NOD mice, treated with DMSO or BB-Cl-amidine, at 13 weeks of age (E) and at 25 weeks of age (F) (n = 9-17 samples per group; two independent experiments were performed, with at least two mice per group per experiment). Data in C, E and F are mean ± SEM and were analyzed by unpaired t-test with Welch's correction. Data in D were analyzed by Mann-Whitney U test. *P<0.05 and **P<0.01.

Figure 4 - BB-Cl-amidine treatment reduces NET release. A-B: Bone marrow-derived neutrophils were isolated from 13-week-old NOD mice treated with DMSO or BB-Cl-amidine and cultured for 3h. Spontaneous NET formation was blindly evaluated by fluorescence microscopy. A: Representative images of spontaneous NETosis of bone marrow-derived neutrophils from DMSO or BB-Cl-amidine treated mice (scale bar = 10µm). White arrows point to NET forming cells. B: Percentage of NET formation was quantified blindly by fluorescence microscopy, after Hoechst staining (n = 10-15 mice per group; two independent

experiments were performed, with at least four mice per group per experiment). Each dot indicates the value for a single mouse. Data in B are mean ± SEM and were analyzed by unpaired t-test with Welch's correction. *P<0.05.

Figure 5 – BB-Cl-amidine alters the phenotype of immune infiltrate in the islets. A: Insulitis score of 13-week-old NOD mice treated with vehicle (DMSO) or BB-Cl-amidine from 8-13 weeks of age (n = 6 mice per group; two independent experiments were performed, with three mice per group per experiment). Score 0 (☐): intact islets; 1 (▥): peri-insulitis; 2 (■): <50% infiltration; 3 (▤): >50% infiltration; and 4 (■): complete destruction. B-C: Immune cells isolated from the pancreas of 13-week-old DMSO or BB-Cl-amidine treated NOD mice were stimulated *in vitro* with PMA and ionomycin in the presence of GolgiStop. Representative flow cytometry plots and percentage of IFNγ$^+$ cells (%IFNγ$^+$) in CD4$^+$ (B) and CD8$^+$ (C) T cells isolated from pancreas (n = 9-12 mice per group; two independent experiments were performed with at least three mice per group per experiment). D-F: Representative flow cytometry plots and percentage of T_{reg} (CD4$^+$ CD25$^+$ Foxp3$^+$) (D), CD4$^+$ T_{EM} (CD4$^+$ Foxp3$^-$ CD44^{HIGH} CD62L$^-$) (E) and CD8$^+$ T_{EM} (CD8$^+$ Foxp3$^-$ CD44^{HIGH} CD62L$^-$) (F) in pancreas of 13-week-old NOD mice treated with DMSO or BB-Cl-amidine (n = 15-16 mice per group; two independent experiments were performed with at least six mice per group per experiment). Data in B-F are mean ± SEM and were analyzed by unpaired t-test with Welch's correction. *P<0.05 and **P<0.01. T_{reg}, regulatory T cells; T_{EM}, effector memory T cells.

Figure 6 - BB-Cl-amidine treatment is associated with a Th1 to Th2 shift in the periphery. A-D: Serum cytokine levels of IFNγ (A), IL-4 (B), IL-10 (C) and ratio IFNγ/IL-10 (D) in 13-week-old NOD mice treated from 8-13 weeks with DMSO or BB-Cl-amidine (n = 28-35 mice per group; four independent experiments were performed with at least seven mice per group per experiment). E-H: Splenocytes isolated from the pancreas of 13-week-old DMSO or BB-Cl-amidine treated NOD mice were stimulated *in vitro* with PMA and ionomycin in the presence of GolgiStop (n = 18-19 mice per group; two independent experiments were performed with at least eight mice per group per experiment). Cytokine production was measured by flow cytometry in CD4$^+$ and CD8$^+$ T cell populations considering the 2 following parameters: 1) percentage of IFNγ$^+$ cells (%IFNγ$^+$) and 2) fold change of the MFI of IFNγ in IFNγ$^+$ cells (MFI IFNγ$^+$). Per experiment, the geometric MFI of each sample was normalized to the average geometric MFI of the DMSO group. Representative flow cytometry plots and histograms depicting the geometric MFI of IFNγ between the two groups are shown above the pooled data. E-F: IFNγ$^+$ (E) and MFI IFNγ$^+$ (F) in splenic CD4$^+$ T cells. G-H: %IFNγ$^+$ (G) and MFI IFNγ$^+$ (H) in splenic CD8$^+$ T cells. Data in A-H are mean ± SEM and were analyzed by unpaired t-test with Welch's correction. *P<0.05, **P<0.01 and ****P<0.0001.

Figure 7 - BB-Cl-amidine increases the frequency of T_{reg} cells in the periphery. Representative flow cytometry plots and percentage of T_{reg} (CD4$^+$ CD25$^+$ Foxp3$^+$), CD4$^+$ T_{EM} (CD4$^+$ Foxp3$^-$ CD44^{HIGH} CD62L$^-$) and CD8$^+$ T_{EM} (CD8$^+$ Foxp3$^-$ CD44^{HIGH} CD62L$^-$) in peripheral blood (A-C) and spleen (D-F) from 13-week-old NOD mice treated with DMSO or BB-Cl-amidine (n = 15-19 mice per group; two independent experiments were performed with at least six mice per group per experiment). Data in A-F are mean ± SEM and were analyzed by unpaired t-test with Welch's correction. *P<0.05 and **P<0.01. T_{reg}, regulatory T cell; T_{EM}, effector memory T cell.

Fig 1

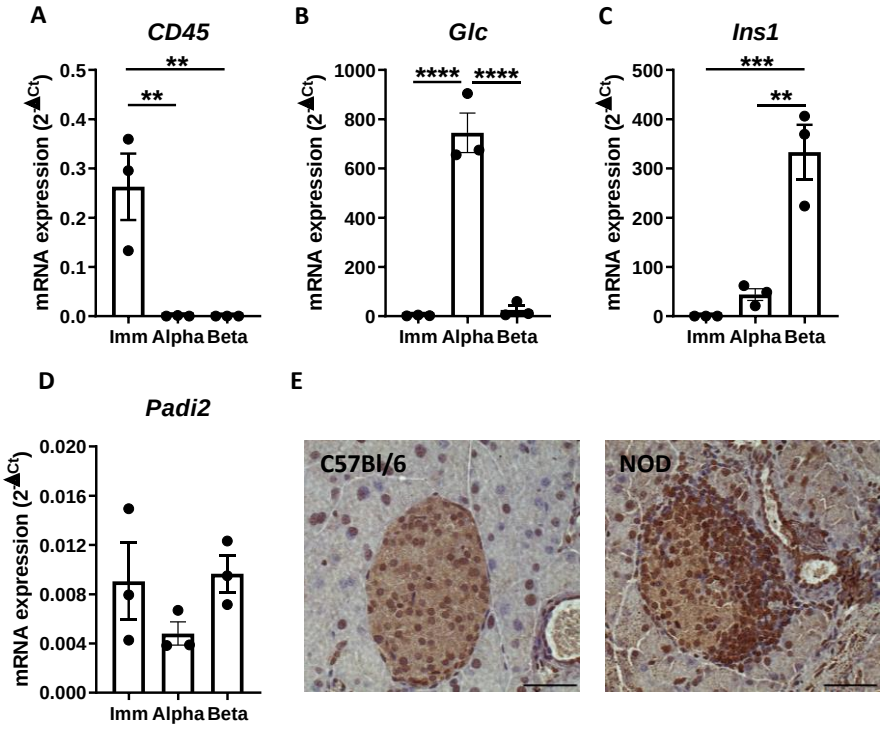
A
CD45
mRNA expression (2^-ΔCt)
0.5
0.4
0.3
0.2
0.1
0.0
**
**
Imm Alpha Beta
B
Glc
mRNA expression (2^-ΔCt)
1000
800
600
400
200
0
****
****
Imm Alpha Beta
C
Ins1
mRNA expression (2^-ΔCt)
500
400
300
200
100
0
***
**
Imm Alpha Beta
D
Padi2
mRNA expression (2^-ΔCt)
0.020
0.016
0.012
0.008
0.004
0.000
Imm Alpha Beta
E
C57Bl/6
NOD

Fig 2

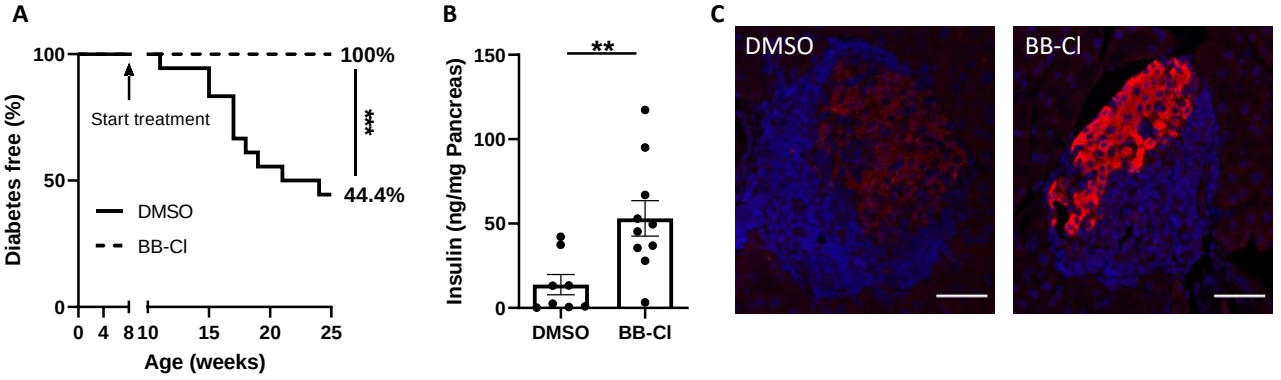
A
100
50
0
Diabetes free (%)
100%
Start treatment
***
44.4%
DMSO
BB-Cl
0 4 8 10 15 20 25
Age (weeks)
B
150
100
50
0
Insulin (ng/mg Pancreas)
**
DMSO
BB-Cl
C
DMSO
BB-Cl

Fig 3

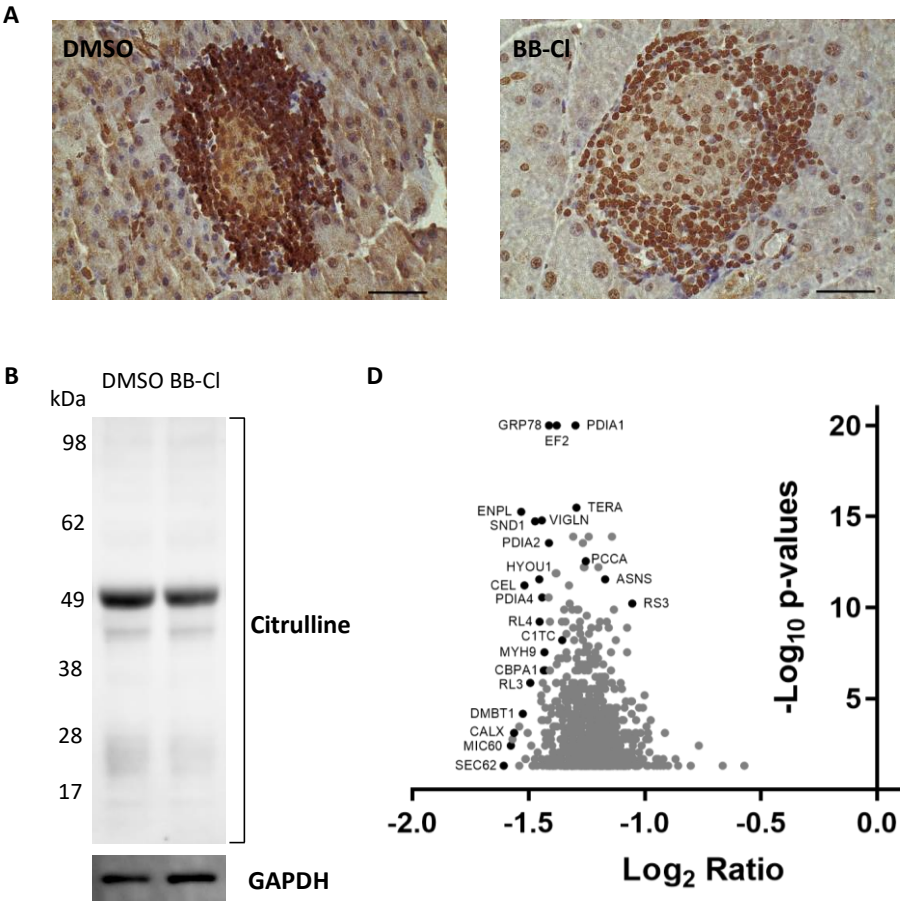
A
DMSO
BB-Cl
B
DMSO BB-Cl
kDa
98
62
49
38
28
17
Citrulline
GAPDH
D
GRP78
PDIA1
EF2
ENPL
TERA
SND1
VIGLN
PDIA2
PCCA
HYOU1
ASNS
CEL
PDIA4
RS3
RL4
C1TC
MYH9
CBPA1
RL3
DMBT1
CALX
MIC60
SEC62
20
15
10
5
-Log10 p-values
-2.0
-1.5
-1.0
-0.5
0.0
Log2 Ratio
C
Density ratio
15
10
5
0
**
DMSO
BB-Cl
E
13 weeks
Ab levels (Signal)
15000
10000
5000
0
*
DMSO
BB-Cl
F
25 weeks
Ab levels (Signal)
15000
10000
5000
0
*
DMSO
BB-Cl

Fig 4

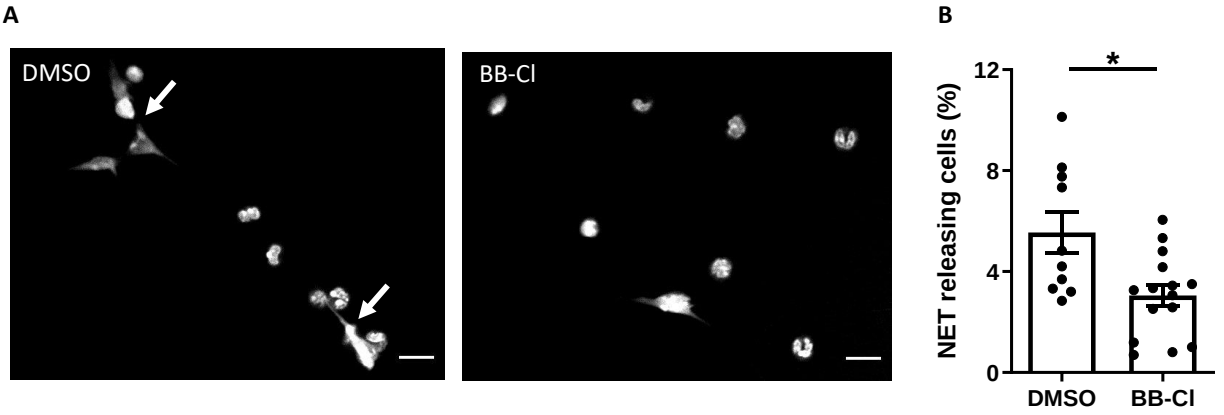

Fig 5

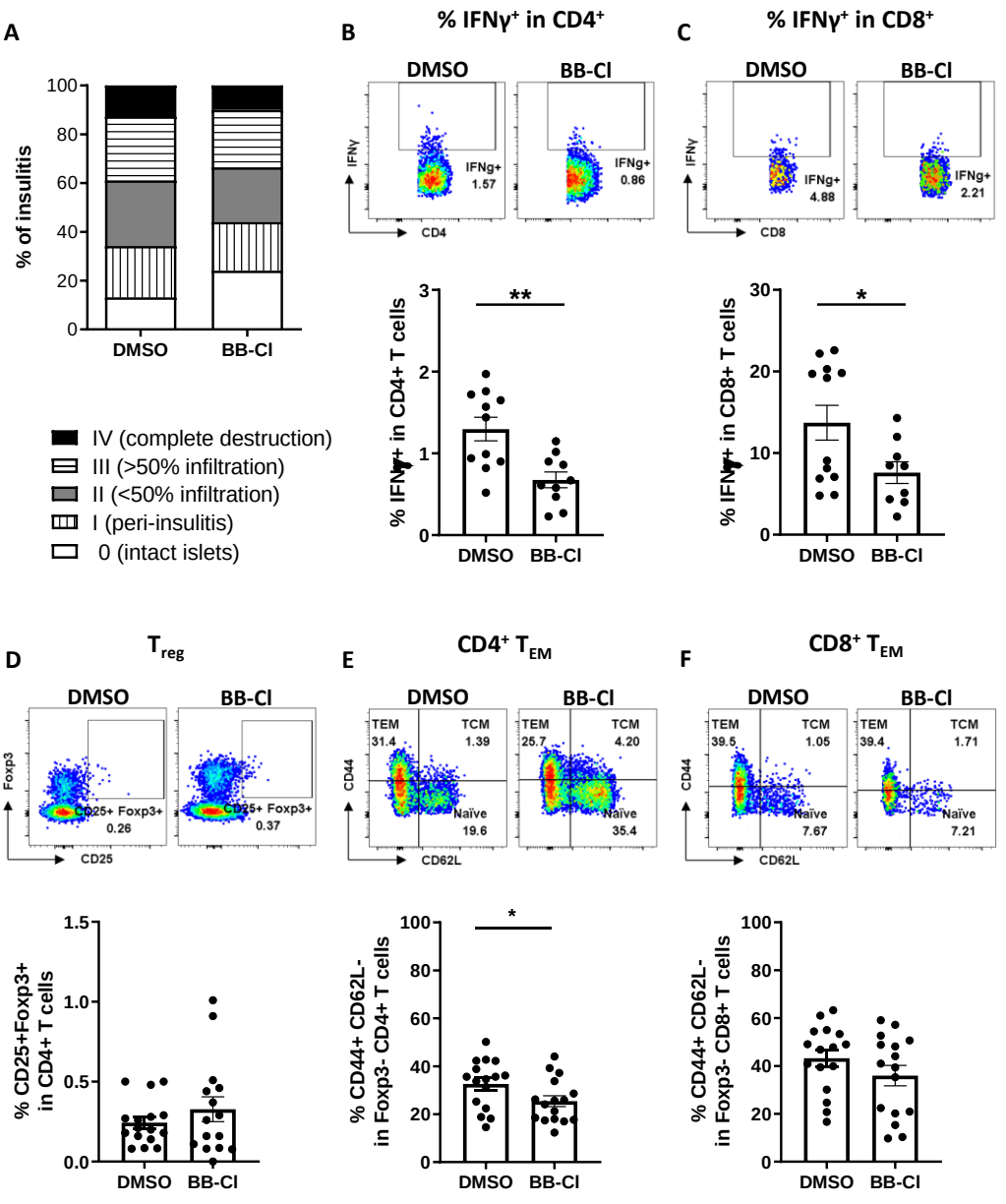
A
% of insulitis
100
80
60
40
20
0
DMSO
BB-Cl
IV (complete destruction)
III (>50% infiltration)
II (<50% infiltration)
I (peri-insulitis)
0 (intact islets)
B
% IFNγ+ in CD4+
DMSO
BB-Cl
IFNγ
CD4
IFNg+
1.57
IFNg+
0.86
% IFNγ+ in CD4+ T cells
**
C
% IFNγ+ in CD8+
DMSO
BB-Cl
IFNγ
CD8
IFNg+
4.88
IFNg+
2.21
% IFNγ+ in CD8+ T cells
*
D
Treg
DMSO
BB-Cl
Foxp3
CD25
CD25+ Foxp3+
0.26
CD25+ Foxp3+
0.37
% CD25+Foxp3+ in CD4+ T cells
E
CD4+ TEM
DMSO
BB-Cl
CD44
CD62L
TEM
31.4
TCM
1.39
Naïve
19.6
TEM
25.7
TCM
4.20
Naïve
35.4
% CD44+ CD62L- in Foxp3- CD4+ T cells
*
F
CD8+ TEM
DMSO
BB-Cl
CD44
CD62L
TEM
39.5
TCM
1.05
Naïve
7.67
TEM
39.4
TCM
1.71
Naïve
7.21
% CD44+ CD62L- in Foxp3- CD8+ T cells

Fig 6

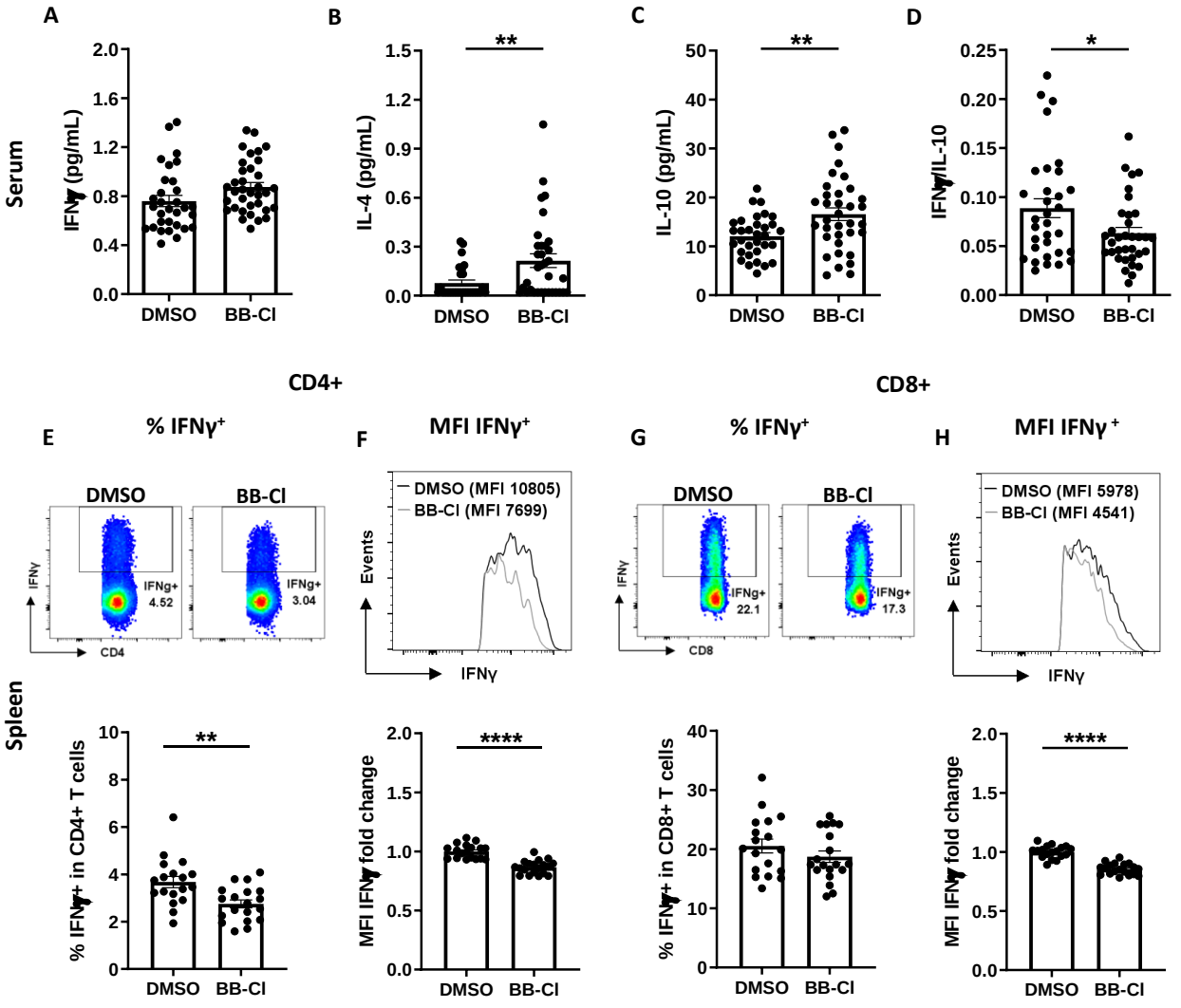
Serum
A
IFNγ (pg/mL)
DMSO
BB-Cl
B
IL-4 (pg/mL)
**
C
IL-10 (pg/mL)
**
D
IFNγ/IL-10
*
CD4+
CD8+
E
% IFNγ+
DMSO
BB-Cl
IFNγ
CD4
IFNg+ 4.52
IFNg+ 3.04
F
MFI IFNγ+
DMSO (MFI 10805)
BB-Cl (MFI 7699)
Events
IFNγ
G
% IFNγ+
CD8
IFNg+ 22.1
IFNg+ 17.3
H
MFI IFNγ +
DMSO (MFI 5978)
BB-Cl (MFI 4541)
Spleen
% IFNγ+ in CD4+ T cells
**
MFI IFNγ fold change
****
% IFNγ+ in CD8+ T cells
MFI IFNγ fold change
****

Fig 7

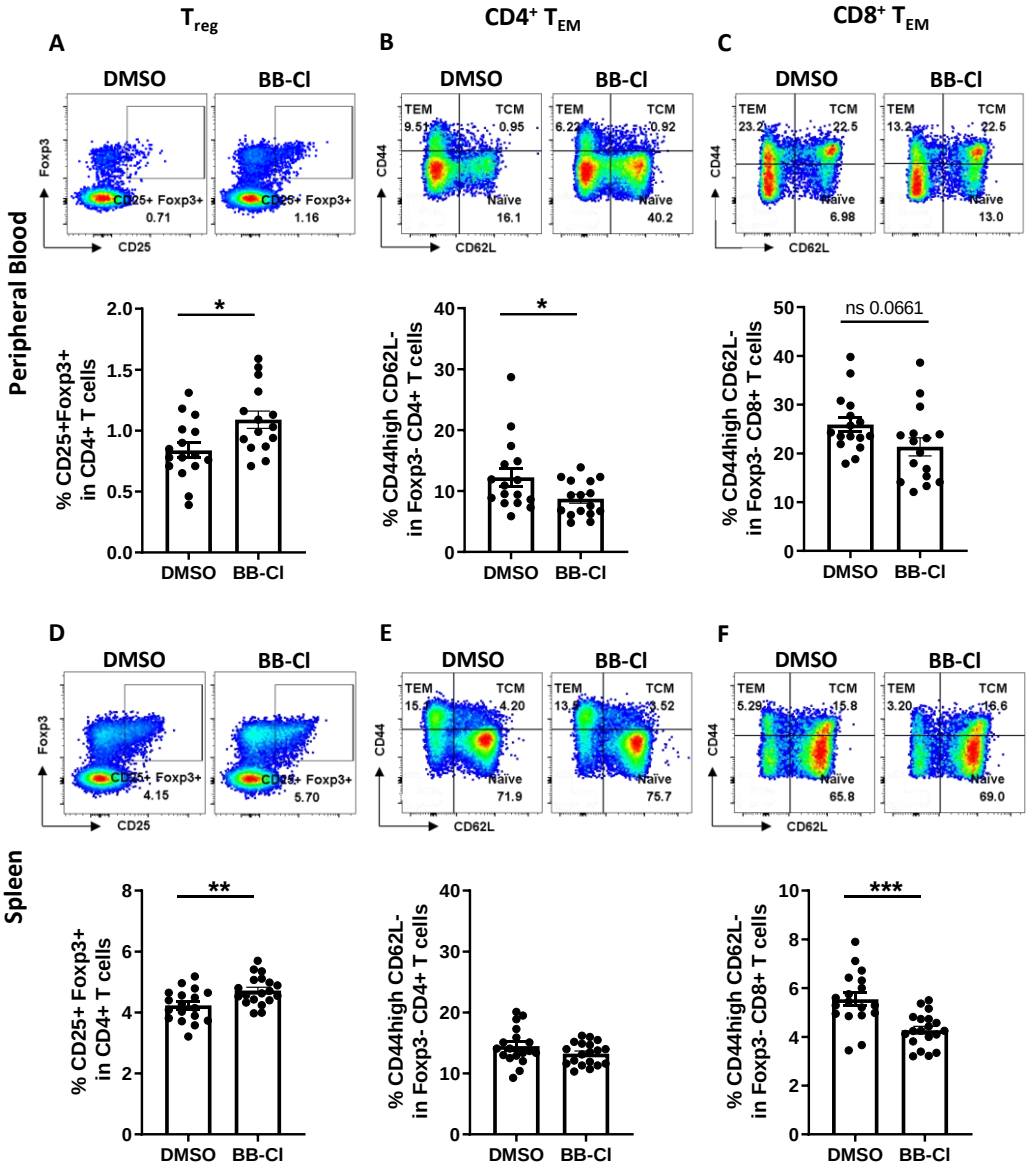
T reg
CD4+ T EM
CD8+ T EM
A
B
C
DMSO
BB-Cl
Peripheral Blood
Foxp3
CD25
CD25+ Foxp3+ 0.71
CD25+ Foxp3+ 1.16
CD44
CD62L
TEM
TCM
Naive
9.51
0.95
16.1
6.22
0.92
40.2
23.2
22.5
6.98
13.2
22.5
13.0
% CD25+Foxp3+ in CD4+ T cells
% CD44high CD62L- in Foxp3- CD4+ T cells
% CD44high CD62L- in Foxp3- CD8+ T cells
*
*
ns 0.0661
D
E
F
Spleen
CD25+ Foxp3+ 4.15
CD25+ Foxp3+ 5.70
4.20
71.9
75.7
5.29
15.8
65.8
3.20
16.6
69.0
% CD25+ Foxp3+ in CD4+ T cells
% CD44high CD62L- in Foxp3- CD4+ T cells
% CD44high CD62L- in Foxp3- CD8+ T cells
**
***

Sup. Fig. 1

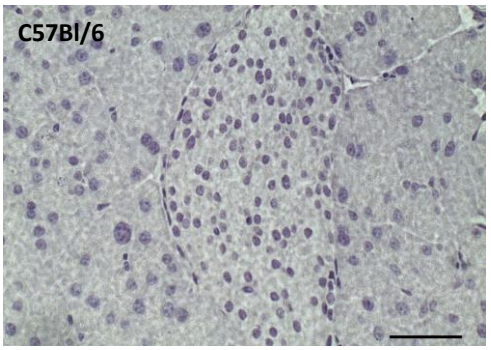

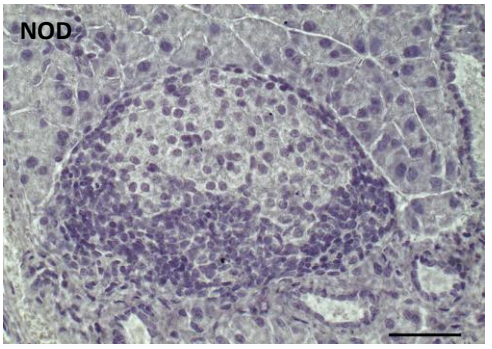

Sup. Fig. 2

A

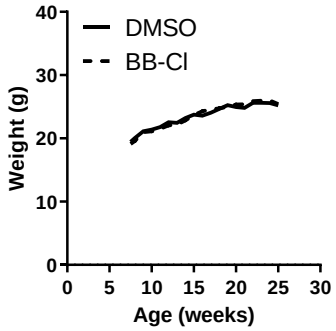

Sup. Fig. 3

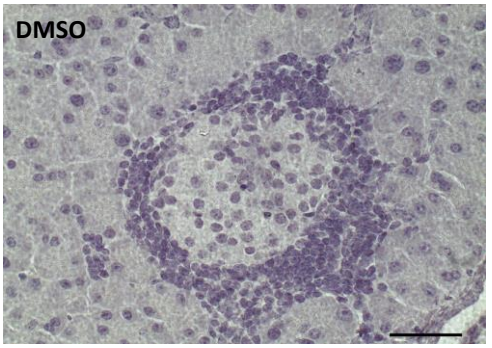

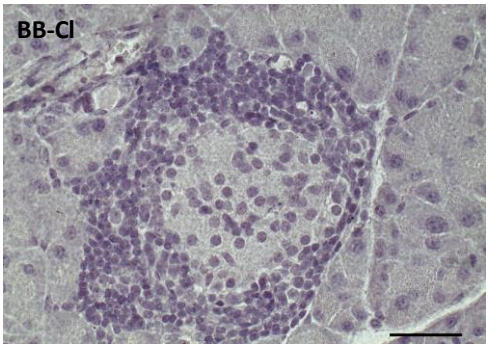

Sup. Fig. 4A

A

Pancreas

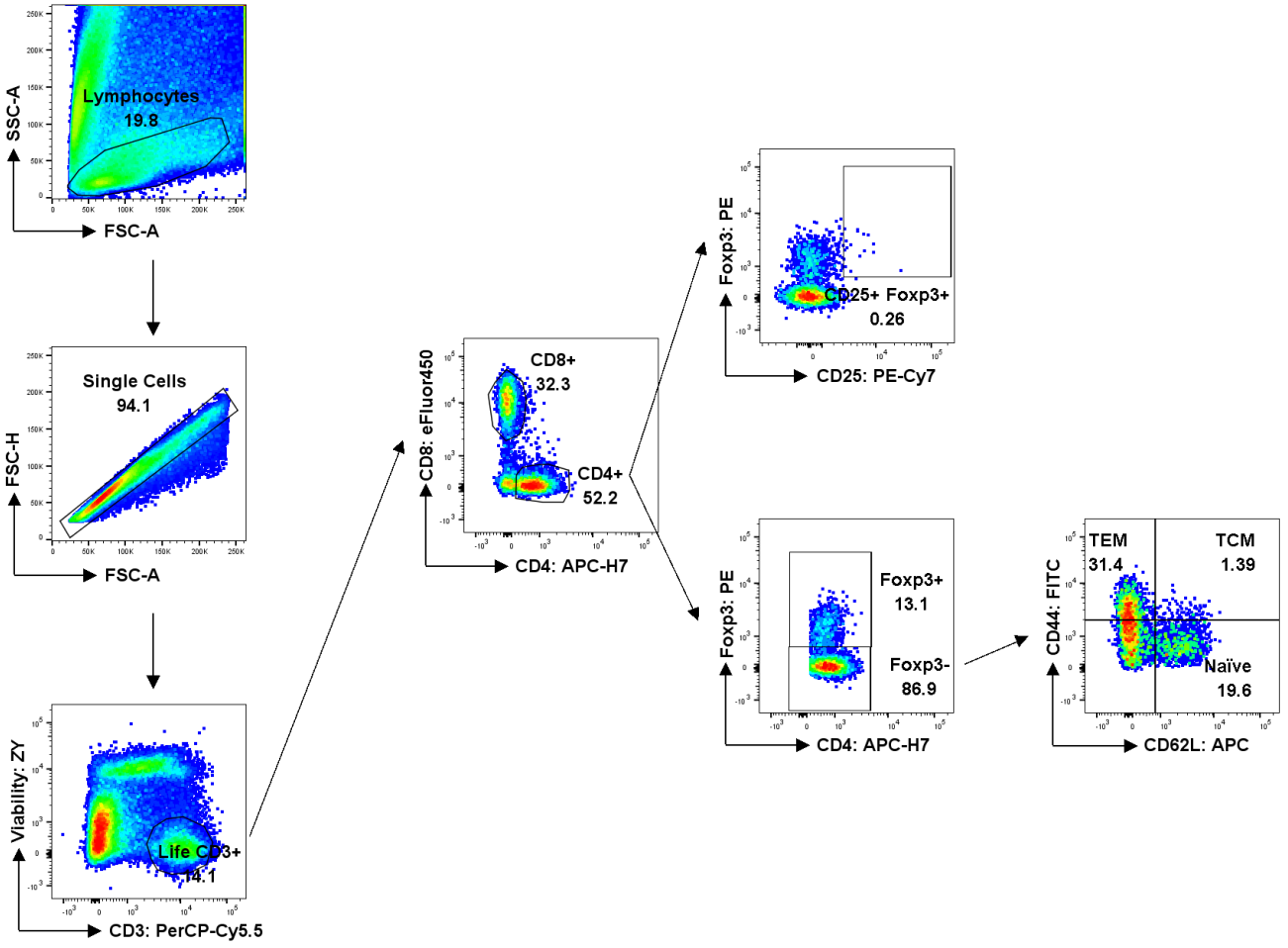

Sup. Fig. 4B

B

Blood

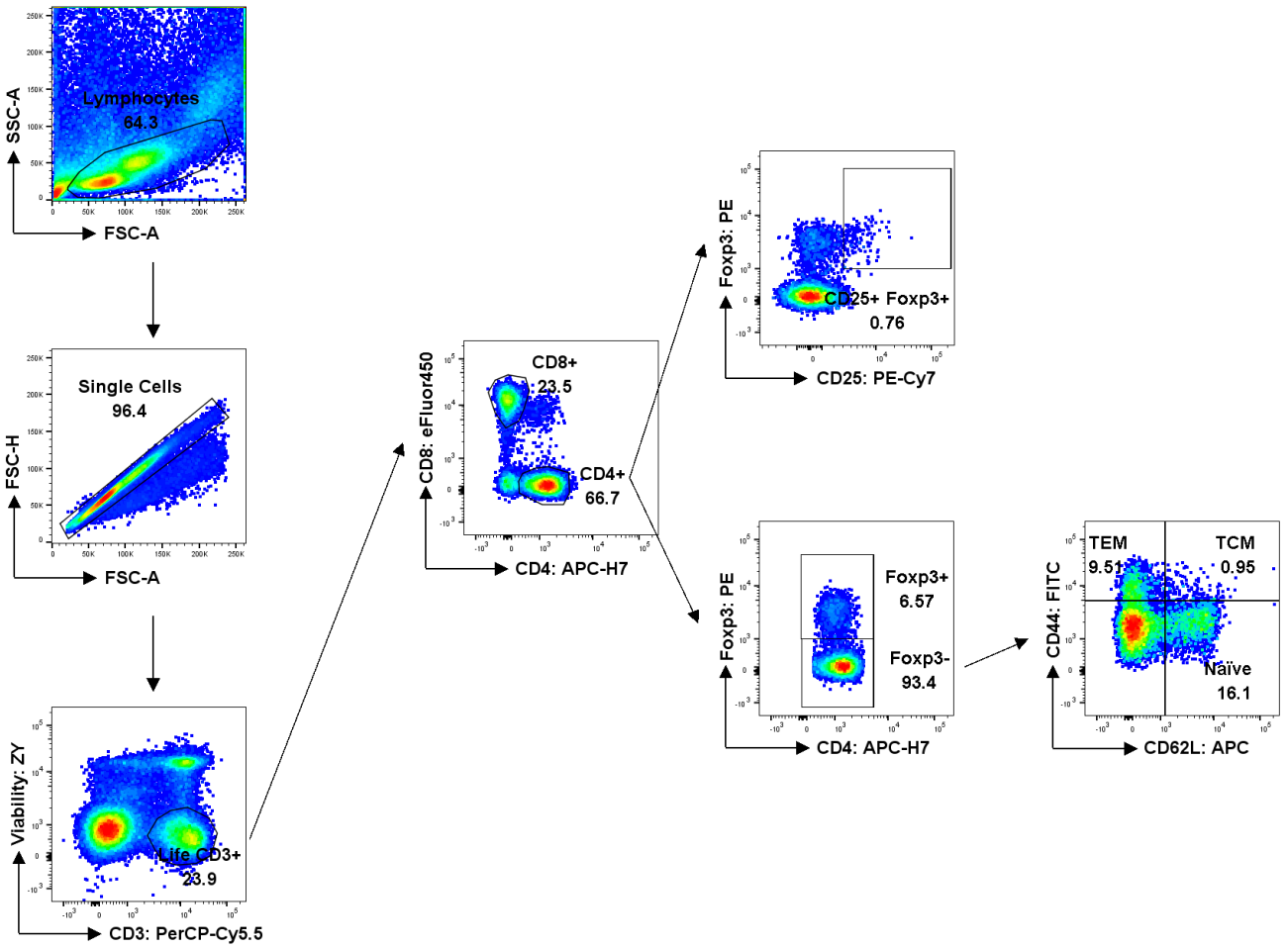

Sup. Fig. 4C

C

Spleen

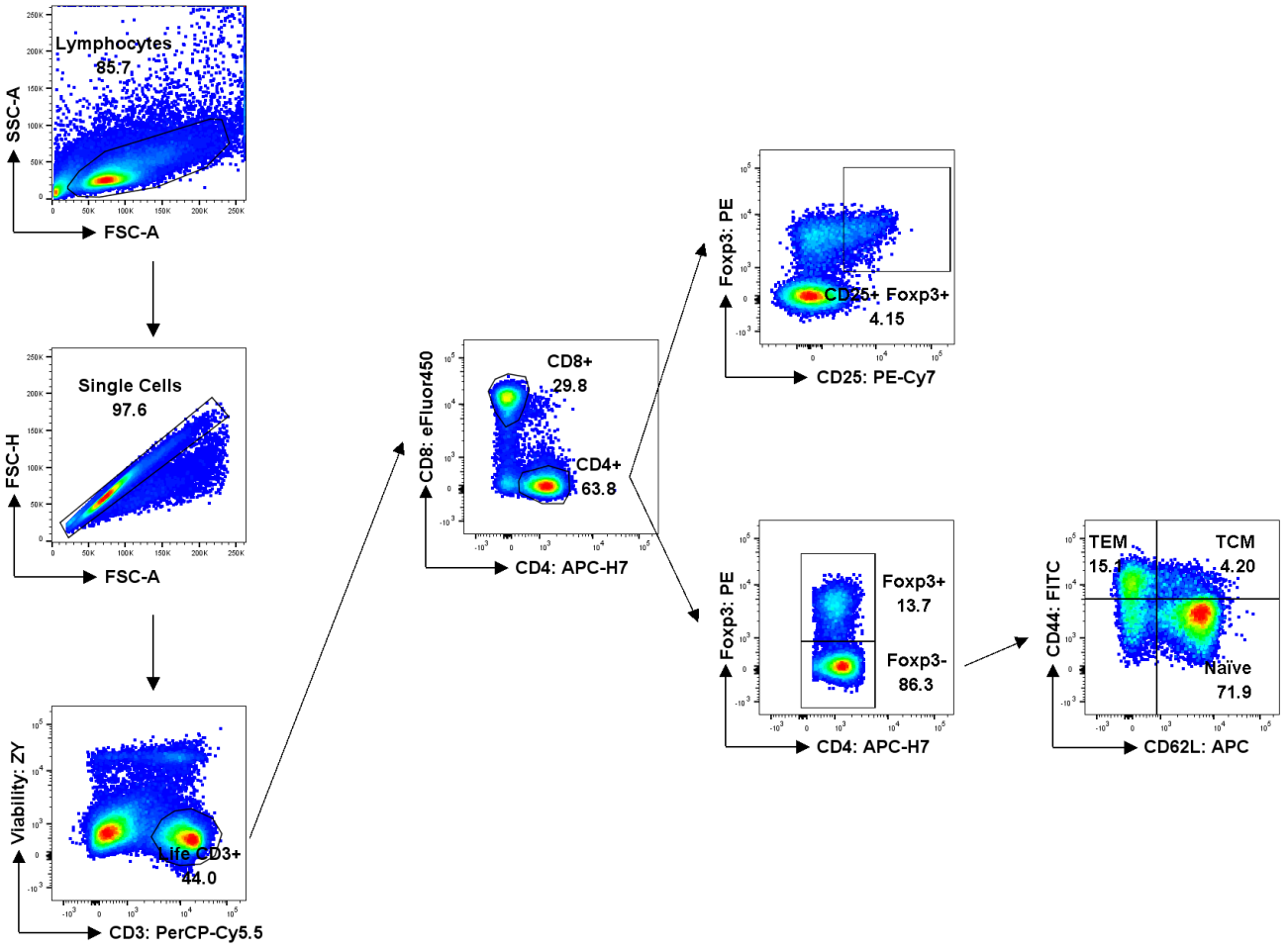

Sup. Fig. 5

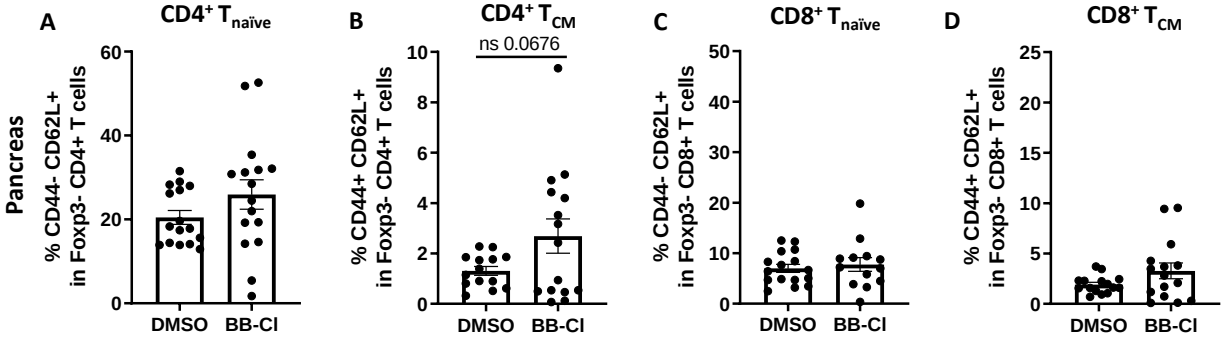
A
CD4+ Tnaïve
Pancreas
% CD44- CD62L+ in Foxp3- CD4+ T cells
60
40
20
0
DMSO
BB-Cl
B
CD4+ TCM
ns 0.0676
% CD44+ CD62L+ in Foxp3- CD4+ T cells
10
8
6
4
2
0
DMSO
BB-Cl
C
CD8+ Tnaïve
% CD44- CD62L+ in Foxp3- CD8+ T cells
50
40
30
20
10
0
DMSO
BB-Cl
D
CD8+ TCM
% CD44+ CD62L+ in Foxp3- CD8+ T cells
25
20
15
10
5
0
DMSO
BB-Cl

Sup. Fig. 6

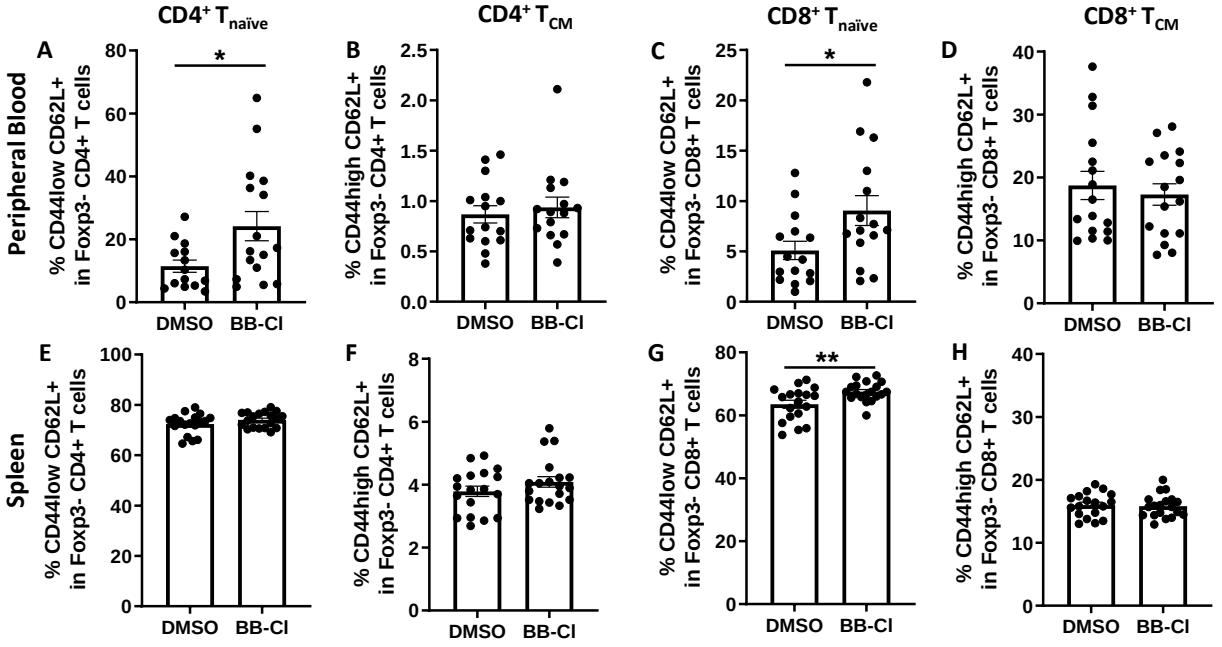
CD4+ Tnaïve
CD4+ TCM
CD8+ Tnaïve
CD8+ TCM
Peripheral Blood
Spleen
A
B
C
D
E
F
G
H
% CD44low CD62L+ in Foxp3- CD4+ T cells
% CD44high CD62L+ in Foxp3- CD4+ T cells
% CD44low CD62L+ in Foxp3- CD8+ T cells
% CD44high CD62L+ in Foxp3- CD8+ T cells
DMSO
BB-Cl
*
**